Stabilization effect of traffic flow in an extended car-following model based on an intelligent transportation system application

H. X. Ge,[1] S. Q. Dai,[1] L. Y. Dong,[1] and Y. Xue[2]
[1]*Shanghai Institute of Applied Mathematics and Mechanics, Shanghai University, Shanghai 200072, China*
[2]*Department of Physics, GuangXi University, Nanning 530004, China*
(Received 21 July 2004; published 23 December 2004)

An extended car following model is proposed by incorporating an intelligent transportation system in traffic. The stability condition of this model is obtained by using the linear stability theory. The results show that anticipating the behavior of more vehicles ahead leads to the stabilization of traffic systems. The modified Korteweg-de Vries equation (the mKdV equation, for short) near the critical point is derived by applying the reductive perturbation method. The traffic jam could be thus described by the kink-antikink soliton solution for the mKdV equation. From the simulation of space-time evolution of the vehicle headway, it is shown that the traffic jam is suppressed efficiently with taking into account the information about the motion of more vehicles in front, and the analytical result is consonant with the simulation one.

DOI: 10.1103/PhysRevE.70.066134 PACS number(s): 05.70.Fh, 05.70.Jk

I. INTRODUCTION

A traffic jam is an important issue from the viewpoint of transportation efficiency and reduction in pollution, which has thus attracted much attention recently. Lots of studies have been conducted with different traffic models, such as the cellular automaton models, car-following models, gas kinetic models and hydrodynamic models (see Refs. [1–8]). In recent years, some researchers have investigated the traffic jam by use of nonlinear analysis. Kurtze and Hong [9] have derived the Korteweg-de Vries (KdV) equation from the hydrodynamic model and showed that the traffic soliton appears near the neutral stability line. Komatsu and Sasa [10] have deduced the modified KdV (mKdV) equation from the optimal velocity model proposed by Bando *et al.* [11,12]. Nagatani [13,14] have derived the mKdV equation based on a hydrodynamic model. For public demand, it is necessary to raise the transportation efficiency and prevent traffic jams. Traffic control systems have been utilized as a part of intelligent transport system (for short, ITS). Drivers can receive information of other vehicles on roads, and then determine the velocity of their own vehicles. In light of this information, it is possible to improve the stability of traffic flow and suppress the appearance of a traffic jam. Several traffic models involving the use of ITS information have been proposed. Helbing [5] presented an improved gas-kinetic traffic model, which differs from others mainly by introducing a nonlocal interaction term that takes into account the space requirements of vehicles and the correlations of successive vehicle velocities. The model reflects the anticipation behavior of drivers, which is responsible for a smoothing effect that acts only in the neighboring backward direction. Nagatani [15] put forward an extended optimal velocity model including the vehicle interaction with the next car ahead (i.e., the next-nearest-neighbor interaction). Xue [3] proposed a lattice model of optimized traffic flow with the consideration of the optimal current with the next-nearest-neighbor interaction. Lenz, Wanger, and Sollacher [16] constructed a model that a driver looks at many vehicles ahead of him/her. Hasebe, Nakayama, and Sugiyama [17,18] presented an extended optimal velocity model applied to a cooperative driving control system. In their models, a driver can adjust the velocity by using the information of an arbitrary number of vehicles that precede or follow. They found that there exist a certain set of parameters that make traffic flow "most stable" in their "forward looking" optimal velocity model. But the dynamic behavior near the critical point has not been investigated. In this paper, an extended car following model with the consideration of an arbitrary number of vehicles ahead on a single-lane highway is presented; and then a linear stability theory is given to show the stabilization effect of the new consideration. Moreover, we apply the nonlinear analysis to derive the mKdV equation near the critical point equation and obtain its kink-antikink soliton solution to describe the traffic jam. Finally numerical simulation is carried out to validate the analytic results.

II. MODEL

An extended car following model is proposed taking into account an arbitrary number of vehicles ahead on a single-lane highway. The vehicle motion is described by the following differential equation:

$$\frac{dx_j(t+\tau)}{dt} = V(\Delta x_j(t), \Delta x_{j+1}(t), \ldots, \Delta x_{j+n-1}(t)), \qquad (1)$$

where $x_j(t+\tau)$ is the position of car j at time $t+\tau$; $\Delta x_j(t) \equiv x_{j+1}(t) - x_j(t)$ is the headway of car j at time t; n denotes the number of vehicles ahead considered; τ is introduced to denote the delay time with which the car velocity reaches the optimal velocity as the traffic flow is varying. We have assumed that a driver can obtain the information of n vehicles in front. The car velocity $dx_j(t+\tau)/dt$ is adjusted according to the vehicle headways $(\Delta x_j(t), \Delta x_{j+1}(t), \ldots, \Delta x_{j+n-1}(t))$

We rewrite Eq. (1) to obtain the difference equation

$$x_j(t+2\tau) - x_j(t+\tau) = \tau V(\Delta x_j(t), \Delta x_{j+1}(t), \ldots, \Delta x_{j+n-1}(t)). \tag{2}$$

We assume the optimal velocity V depending on the vehicle headways $(\Delta x_j(t), \Delta x_{j+1}(t), \ldots, \Delta x_{j+n-1}(t))$ in the following collective way:

$$V = V\left(\sum_{l=1}^{n} \beta_l \Delta x_{j+l}(t)\right), \tag{3}$$

in which β_l is the weighted function of $\Delta x_{j+l}(t)$, which corresponds to sensitivity α_i in a multianticipative car-following model [16]. The difference between them lies in the fact that the optimal velocity in Ref. [16] is related to a certain position, while in this paper the vehicles ahead are regarded as a whole and the nonlocal effect is considered. It is necessary to point out that β_l $(l=1,2,\ldots,n)$ have the following properties.

(1) β_l $(l=1,2,\ldots,n)$ decrease monotonically with increasing l, which means $\beta_l/\beta_{l-1}<1$, for we know that the influence of the vehicles ahead on the vehicle motion reduces gradually as the distance between the considered vehicle and the vehicle ahead increases.

(2) $\Sigma_{l=1}^{n}\beta_l=1$, and $\beta_l=1$ for $n=1$. In this paper, we take tentatively for $n>1$

$$\beta_l = \begin{cases} \dfrac{6}{7^l}, & l \neq n \\ \dfrac{1}{7^{n-1}}, & l = n. \end{cases} \tag{4}$$

It is convenient to rewrite Eq. (2) in terms of the headway, which reads

$$\Delta x_j(t+2\tau) - \Delta x_j(t+\tau) = \tau\left[V\left(\sum_{l=1}^{n}\beta_l \Delta x_{j+l}(t)\right) - V\left(\sum_{l=1}^{n}\beta_l \Delta x_{j+l-1}(t)\right)\right]. \tag{5}$$

The optimal velocity is selected similar to that used by Bando *et al.* [12]

$$V(\Delta x_j(t), \Delta x_{j+1}(t), \ldots, \Delta x_{j+n-1}(t)) = \frac{v_{max}}{2}\left\{\tanh\left(\sum_{l=1}^{n}\beta_l \Delta x_{j+l-1}(t) - h_c\right) + \tanh(h_c)\right\}, \tag{6}$$

where h_c is the safety distance, and Eq. (6) has the inflection point at $\Sigma_{l=1}^{n}\beta_l \Delta x_{j+l-1}(t)=h_c$. We name $\Sigma_{l=1}^{n}\beta_l \Delta x_{j+l-1}(t)$ as the weighted headway. When the weighted headway is less than the safety distance, the vehicle velocity is reduced to prevent crashing into the preceding vehicle. On the other hand, if it is larger than the safety distance, the vehicle velocity increases to the maximum velocity. The reason we choose the form of Bando *et al.*, other than that of Whitham [19], lies in the fact that the former has a turning point, which is important for us to derive the mKdV equation from Eq. (5).

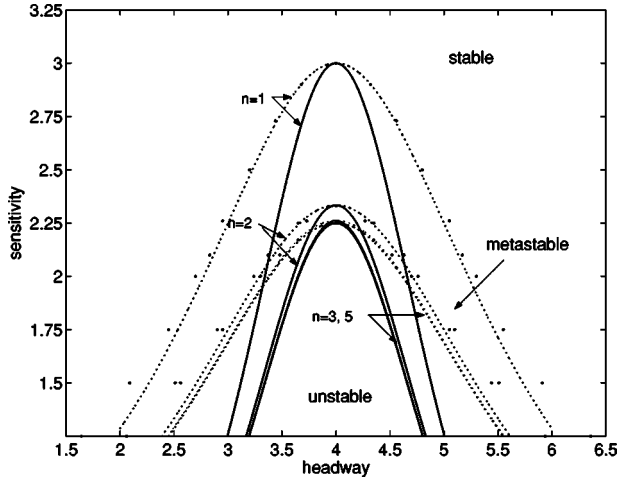

FIG. 1. Phase diagram in the headway-sensitivity space. The solid lines represent the neutral stability curves for $n=1,2,3,5$. The dotted lines indicate the coexisting curves for $n=1,2,3,5$. The solid circles show the simulation results for $n=1,2,5$. ($v_{max}=2.0$, $h_c=4.0$).

III. LINEAR STABILITY ANALYSIS

The method of linear stability analysis is applied to the extended car following model. It is obvious that the vehicle moves with the constant headway h and the optimal velocity $V(h,h,\ldots,h)$ is the steady-state solution for Eq. (5), given as

$$x_j^0(t) = hj + V(h,h,\ldots,h)t \text{ with } h = \frac{L}{N}, \tag{7}$$

where N is the total number of vehicles, and L is the road length.

Suppose $y_j(t)$ to be a small deviation from the steady-state solution $x_j^0(t)$: $x_j(t)=x_j^0(t)+y_j(t)$. Substituting it into Eq. (5) and linearizing the resulting equation yield

$$\Delta y_j(t+2\tau) - \Delta y_j(t+\tau) = \tau V'(h)\left[\sum_{l=1}^{n}\beta_l(\Delta y_{j+l}(t) - \Delta y_{j+l-1}(t))\right], \tag{8}$$

where $\Delta y_j(t) \equiv y_{j+1}(t) - y_j(t)$, and $V'(h) = dV(\Delta x_j)/d\Delta x_j|_{\Delta x_j=h}$.

Expanding y_j in the Fourier-modes: $\Delta y_j(t)=A\exp(ikj+zt)$, we obtain

$$e^{2z\tau} - e^{z\tau} - \tau V'\left[\sum_{l=1}^{n}\beta_l(e^{ikl} - e^{ik(l-1)})\right] = 0. \tag{9}$$

For simplicity, $V'(h)$ is indicated as V' in the above equation and hereafter. Expanding $z=z_1(ik)+z_2(ik)^2+\cdots$ and inserting it into Eq. (9) lead to the first- and second-order terms of coefficients in the expression of z, respectively,

$$z_1 = V' \text{ and } z_2 = -\frac{3}{2}\tau V'^2 + \frac{V'}{2}\sum_{l=1}^{n}\beta_l(2l-1). \tag{10}$$

Thus the neutral stability condition is given by

$$\tau = \frac{\sum_{l=1}^{n} \beta_l (2l-1)}{3V'}. \tag{11}$$

For small disturbances with long wavelengths, the uniform traffic flow is unstable in the condition that

$$\tau > \frac{\sum_{l=1}^{n} \beta_l (2l-1)}{3V'}. \tag{12}$$

The neutral stability line in the parameter space $(\Delta x, a)$ is shown in Fig. 1 by the solid line, where $a=1/\tau$. There exist the critical points (h_c, a_c) for the neutral stability lines as $n=1,2,3,5$, respectively, such that the uniform state irrespective of vehicle headway is always linearly stable for $a>a_c$, while uniform states in a neighborhood of h_c are unstable for $a<a_c$. For the case of $n=1$, the neutral stability line is consistent with those of the original car-following model in single-lane highway traffic flow [20]. The apex of each curve indicates the critical point. The traffic flow is stable above the neutral stability line and a traffic jam will not appear. While below the line, traffic flow is unstable and the density waves emerge. From Fig. 1 it can be seen that with taking into account more vehicles ahead, the critical points and the neutral stability curves are lowered, which means the stability of the uniform traffic flow has been strengthened. The traffic jam is thus suppressed efficiently.

IV. NONLINEAR ANALYSIS

We apply the reductive perturbation method to Eq. (5) and focus on the system behavior near the critical point (h_c, a_c). With such treatment, the nature of kink-antikink soliton solutions can be described by the mKdV equation. We introduce slow scales for space variable j and time variable t [21,22], and define the slow variables X and T as

$$X = \varepsilon(j + bt) \text{ and } T = \varepsilon^3 t, \quad 0 < \varepsilon \ll 1, \tag{13}$$

where b is a constant to be determined. Let

$$\Delta x_j(t) = h_c + \varepsilon R(X,T). \tag{14}$$

Substituting Eqs. (13) and (14) into Eq. (5) and making the Taylor expansions to the fifth order of ε lead to the expression

$$\begin{aligned}
&\varepsilon^2(b-V')\partial_x R + \varepsilon^3\left[\frac{3}{2}b^2\tau - \frac{V'}{2}\sum_{l=1}^{n}\beta_l(2l-1)\right]\partial_x^2 R \\
&+ \varepsilon^4\left\{\partial_T R + \left[\frac{7b^3\tau^2}{6} - \frac{V'}{6}\sum_{l=1}^{n}\beta_l(3l^2-3l+1)\right]\partial_x^3 R \right. \\
&\left. - \frac{V'''}{6}\partial_x R^3\right\} + \varepsilon^5\left\{3b\tau\partial_X\partial_T R + \left[\frac{5}{8}b^4\tau^3 - \frac{V'}{24}\sum_{l=1}^{n}\beta_l(4l^3\right.\right. \\
&\left. - 6l^2 + 4l - 1)\right]\partial_X^4 R - \frac{V'''}{4}\sum_{l=1}^{n}\beta_l(2l-1)[R^2\partial_X^2 R \\
&\left.\left. + 2R(\partial_X R)^2]\right\} = 0,
\end{aligned} \tag{15}$$

where $V' = dV(\Delta x_j)/d\Delta x_j|_{\Delta x_j = h_c}$ and $V''' = d^3V(\Delta x_j)/d\Delta x_j^3|_{\Delta x_j = h_c}$. V' and V''' correspond to $V'(h_c)$, $V'''(h_c)$ in the above equation and hereafter. Near the critical point (h_c, a_c), $\tau=(1+\varepsilon^2)\tau_c$, taking $b=V'$ and eliminating the second- and third-order terms of ε from Eq. (15) result in the simplified equation:

$$\begin{aligned}
&\varepsilon^4\left\{\partial_T R + \left[\frac{7b^3\tau_c^2}{6} - \frac{V'}{6}\sum_{l=1}^{n}\beta_l(3l^2-3l+1)\right]\partial_x^3 R - \frac{V'''}{6}\partial_x R^3\right\} \\
&+ \varepsilon^5\left\{\frac{3}{2}b^2\tau_c\partial_X^2 R - \frac{V'''}{4}\left[\sum_{l=1}^{n}\beta_l(2l-1) - 6b\tau_c\right][R^2\partial_X^2 R \right. \\
&+ 2R(\partial_X R)^2] + \left[-\frac{23}{8}b^4\tau_c{}^3 + \frac{b\tau_c V'}{2}\sum_{l=1}^{n}\beta_l(3l^2-3l+1)\right. \\
&\left.\left. - \frac{V'}{24}\sum_{l=1}^{n}\beta_l(4l^3-6l^2+4l-1)\right]\partial_X^4 R\right\} = 0.
\end{aligned} \tag{16}$$

In order to obtain the standard mKdV equation with higher order correction, we make the following transformations for Eq. (16):

$$T' = -\left[\frac{7b^3\tau_c^2}{6} - \frac{V'}{6}\sum_{l=1}^{n}\beta_l(3l^2-3l+1)\right]T, \tag{17}$$

$$R = \left[\frac{7b^3\tau_c^2}{V'''} - \frac{V'}{V'''}\sum_{l=1}^{n}\beta_l(3l^2-3l+1)\right]^{1/2} R'. \tag{18}$$

Thus we obtain the regularized equation

$$\partial_{T'} R' = \partial_X^3 R' - \partial_X R'^3 - \varepsilon M[R'], \tag{19}$$

where

$$\begin{aligned}
M[R'] = &\frac{9b^2\tau_c}{7b^3\tau_c^2 - V'\sum_{l=1}^{n}\beta_l(3l^2-3l+1)}\partial_X^2 R' + \left[\frac{3}{2}\sum_{l=1}^{n}\beta_l(2l-1) - 9b\tau_c\right][R'^2\partial_X^2 R' + 2R'(\partial_X R')^2] \\
&+ \frac{69b^4\tau_c{}^3 + V'\sum_{l=1}^{n}\beta_l(4l^3-6l^2+4l-1) - 12b\tau_c V'\sum_{l=1}^{n}\beta_l(3l^2-3l+1)}{28b^3\tau_c{}^2 - 4V'\sum_{l=1}^{n}\beta_l(3l^2-3l+1)}\partial_X^4 R'.
\end{aligned} \tag{20}$$

TABLE I. The critical sensitivity a_c and the propagation velocity c.

n	1	2	3	4	5	6	7	8
a_c	3	2.3333	2.26154	2.25164	2.25023	2.25003	2.25	2.25
c	27	29.4	29.8329	29.897	29.9062	29.9075	29.9077	29.9077

Equation (19) is the modified KdV equation with an $O(\varepsilon)$ correction term on the right-hand side. First, we ignore the $O(\varepsilon)$ term in Eq. (19) and get the mKdV equation with the kink-antikink soliton solution

$$R_0'(X,T') = \sqrt{c}\tanh\sqrt{\frac{c}{2}(X-cT')}. \tag{21}$$

Next, supposing $R'(X,T')=R_0'(X,T')+\varepsilon R_1'(X,T')$, we take into account the $O(\varepsilon)$ correction. To determine the selected value of the propagation velocity for the kink-antikink soliton solution[21], it is necessary to consider the solvability condition [22–24]

$$(R_0', M[R_0']) \equiv \int_{-\infty}^{+\infty} dX R_0'\ M[R_0']), \tag{22}$$

where

$$M[R_0'] = M[R'].$$

By performing the integration, we obtain the selected velocity c,

$$c = \frac{-270\sum \beta_l(2l-1)}{\sum \beta_l(10-15l+135l^2+36l^3) - 150\left(\sum \beta_l l\right)^2 - 378\left(\sum \beta_l l^{3/2}\right)^2 + 352\left(\sum \beta_l l\right)^3}, \tag{23}$$

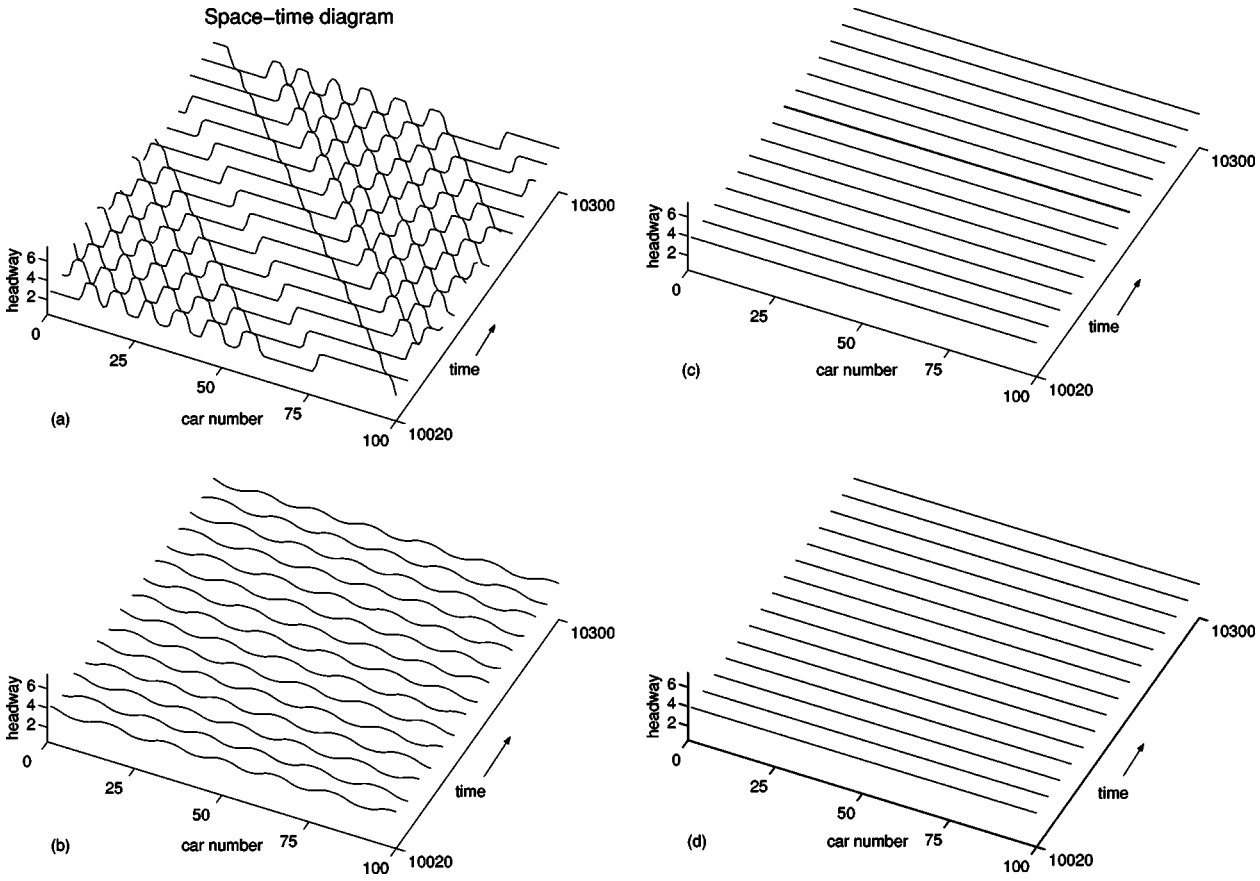

FIG. 2. Space-time evolution of the headway after $t=10\,000$. The patterns (a), (b) for the coexisting phase, and (c), (d) for the freely moving phase. The patterns (a), (b), (c), (d) corresponde to $n=1$, 2, 3, and 5, respectively ($a=2.26$ and $v_{max}=2.0$).

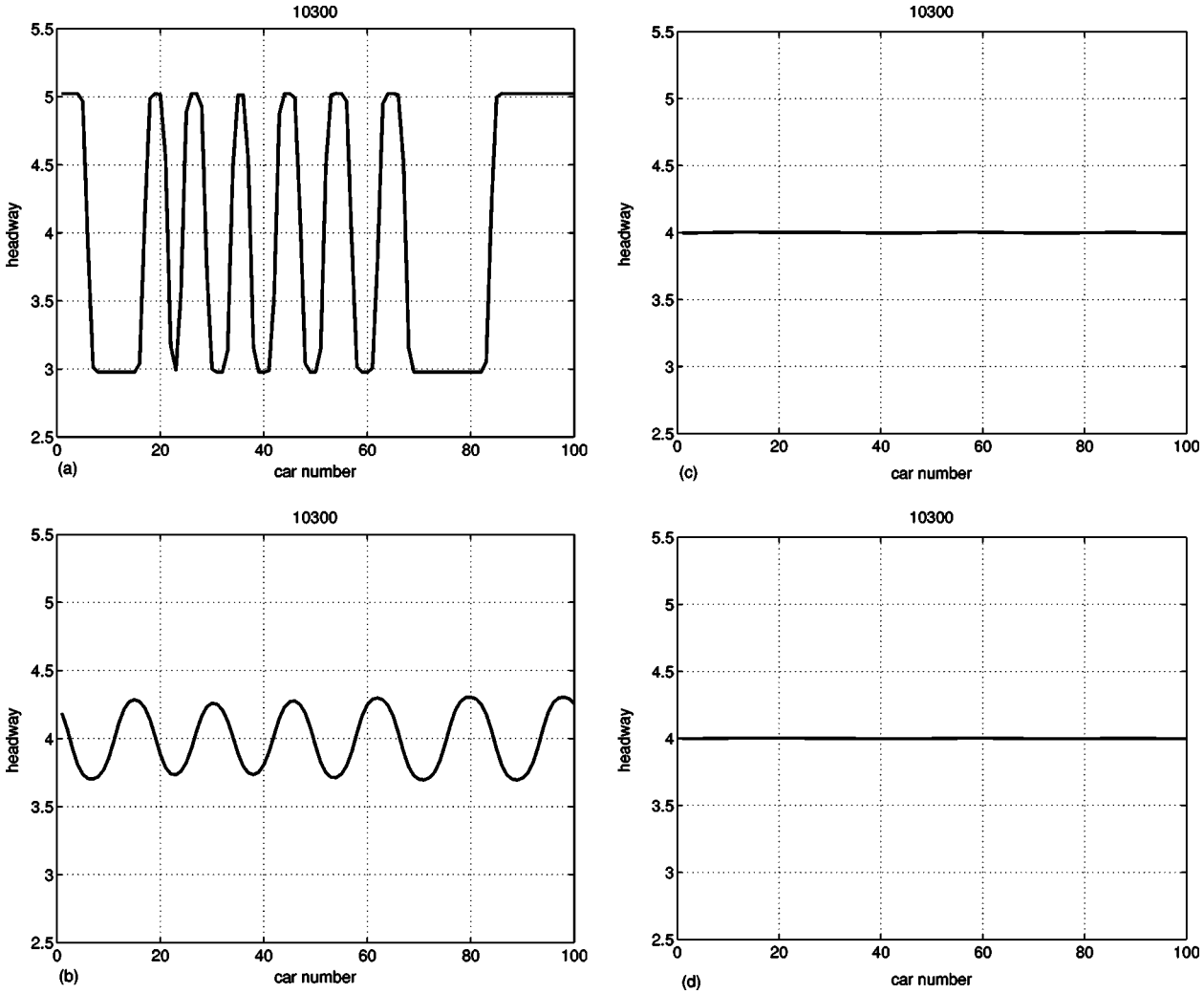

FIG. 3. Headways profile of the density waves at $t=10\,300$. The patterns (a), (b), (c), and (d) corresponde to $n=1$, 2, 3, and 5, respectively ($a=2.26$ and $v_{max}=2.0$).

where Σ denotes $\Sigma_{l=1}^{n}$. Hence we obtain the kink-antikink soliton solution ($V'=1, V'''=-2$),

$$R(X,T)=\left[-\frac{7b^3{\tau_c}^2c}{2}+\frac{c}{2}\sum_{l=1}^{n}\beta_l(3l^2-3l+1)\right]^{1/2}\tanh\sqrt{\frac{c}{2}}\times\left\{X+c\left[\frac{7b^3{\tau_c}^2}{6}-\frac{1}{6}\sum_{l=1}^{n}\beta_l(3l^2-3l+1)\right]T\right\}, \tag{24}$$

where b, τ_c, and c are given before.

V. RESULT ANALYSIS AND NUMERICAL SIMULATION

On the basis of the linear and nonlinear analysis, we obtain the critical point (h_c,a_c) and the propagation velocities c of the kink-antikink soliton solution. We calculate the values of the critical sensitivity a_c and the propagation velocities c by use of Eq. (4), which are listed in Table I. Table I shows that the propagation velocity c increases with increasing n. The critical sensitivity a_c decreases with increasing n, and the stability regions are enlarged for the new model. As n raises up to a certain value, the critical sensitivity a_c and the propagation velocities c will not change further. In fact, only the former three terms play an important role in the stability. We may consider this state as the optimal state and the system is steady. The information of this state is enough for a driver to control the velocity of his/her car. As $n=1$, which corresponds to the case of the first value of weighted function being 1 and the others being 0, the stability region is the smallest, and the result is exactly consistent with that in [15]. So considering the cooperative driving behavior will stabilize the traffic flow.

Computer simulation has been carried out for the extended car following model described by Eq. (5). The boundary conditions selected are periodic ones. The initial conditions are chosen as follows: $\Delta x_j(0)=\Delta x_0=4.0$, $\Delta x_j(1)=\Delta x_0=4.0$ for $j\neq 50,51$, $\Delta x_j(1)=4.0-0.5$ for $j=50$, and $\Delta x_j(1)=4.0+0.5$ for $j=51$, where the total number of cars is $N=100$ and the safety distance is $h_c=4.0$. Figure 1 shows the phase diagram in the space $(\Delta x,a)$ for $n=1,2,3,5$. In the phase diagram, the solid lines represent the neutral stability lines; the dotted lines indicate the coexisting curves

obtained from the solution of the modified KdV equation; and the solid circles show the simulation results. The traffic flow is divided into three regions by the solid line and the dotted line: the first is the stable region above the coexisting curve, the second is the metastable region between the stability line and the coexisting line, and the third is the unstable region below the stability line. We can see that the theoretical results agree with the simulation outcomes and the coexisting curves decrease with increasing values of n. As $n=3$ and 5, the curves related to the neutral stability lines and the coexisting lines are almost coincided, which further demonstrates that considering three cars in front (i.e., $n=3$) is enough for a driver. In fact, this number of cars is closely related to the selection of the weighting function. With a weighting function other than that given in Eq. (4), a slightly different result will be obtained. But we know the behavior of vehicles farther from a considered vehicle will have less influence on it, so the selection in Eq. (4) seems reasonable.

Figure 2 shows the space-time evolution of the headway for various cars in front and the different values of sensitivity. The patterns (a), (b), (c), and (d) in Fig. 2 exhibit the time evolution of the headway profile for $n=1$, 2, 3, and 5, where $v_{max}=2$, $a=2.26$. In patterns (a) and (b), the traffic flow is unstable because the instability condition (12) is satisfied for $n=1,2$ in the condition that $a=2.26$. When small disturbances are added to the uniform traffic flow, they are amplified with time and the uniform flow changes finally to inhomogeneous traffic flow. In patterns (c) and (d), the traffic flow is stable for $n=3,5$ with the same sensitivity, which shows that only considering the next-nearest-neighbor interaction is not enough for suppressing the traffic jam in this situation. The influence of cars in front is almost invariant after $n=3$, which is consistent with the neutral stability lines and coexisting curves in Fig. 1. From Fig. 2 we can see that,in the instability region [see pattern (a) in Fig. 2], the kink-antikink soliton solution appears as traffic jams and the density waves propagate backwards in patterns (a) and (b). Figure 3 shows the headway profile obtained at sufficiently large time $t=10\,300$. With the same sensitivity, as the considered number of cars in front increases, the amplitude of the density wave decreases. In patterns (c) and (d) the density waves disappear and traffic flow is uniform over the whole space. Therefore the simulation outcomes are in agreement with analytical results.

VI. SUMMARY

We have proposed the extended car following model of traffic flow for the purpose of constructing a cooperative driving system for highway traffic and given a form of optimal velocity function taking into account the nonlocal effect. The traffic nature has been analytically analyzed by using the linear and nonlinear analysis. It has been shown that there exists critical point in the model and the neutral stability line is obtained. Obviously, multivehicle consideration could further stabilize traffic flow. The mKdV equation has been derived to describe the traffic behavior near the critical point. Moreover, we gave an example to show the results clearly. As $n=1$, the result is consistent with that in previous work. The results of numerical simulation are presented to illustrate the theoretical conclusion. The simulation results confirm the stability analysis for the extended car-following model and give the optimal state as $n=3$, that is to say, only the information of three cars ahead is enough for cooperative driving. The theoretical results of the coexisting curves are in good agreement with the simulation results.

ACKNOWLEDGMENT

This work was supported by the National Natural Science Foundation of China (Grant Nos. 10202012, 10362001, and 19932020).

[1] D. Chowdhury, L. Santen, and A. Schadschneider, Phys. Rep. **329**, 199 (2000).
[2] K. Nishinari and D. Takahashi, J. Phys. A **33**, 7709 (2000).
[3] Y. Xue, Acta Phys. Sin. **53**, 25 (2004).
[4] Y. Xue, L. Y. Dong, and S. Q. Dai, Acta Phys. Sin. **50**, 444 (2001) (in Chinese).
[5] D. Helbing, A. Hennecke, V. Shvetsov, and M. Treiber, Transp. Res., Part B: Methodol. **35**, 183 (2001).
[6] H. X. Ge, L. Y. Dong, S. Q. Dai, and L. Lei, J. Shanghai Univ. **8**, 1 (2004).
[7] D. Helbing and M. Treiber, Phys. Rev. Lett. **81**, 3042 (1998).
[8] D. Helbing, Phys. Rev. E **53**, 2366 (1996).
[9] D. A. Kurtze and D. C. Hong, Phys. Rev. E **52**, 218 (1995).
[10] T. Komatsu and S. Sasa, Phys. Rev. E **52**, 5574 (1995).
[11] M. Bando, K. Hasebe, A. Nakayama, A. Shibata, and Y. Sugiyama, Jpn. J. Ind. Appl. Math. **11**, 203 (1994).
[12] M. Bando, K. Hasebe, A. Nakayama, A. Shibata, and Y. Sugiyama, Phys. Rev. E **51**, 1035 (1995).
[13] T. Nagatani, Physica A **261**, 599 (1998).
[14] T. Nagatani, Physica A **265**, 297 (1999).
[15] T. Nagatani, Phys. Rev. E **60**, 6395 (1999).
[16] H. Lenz, C. K. Wagner, and R. Sollacher, Eur. Phys. J. B **7**, 331 (1998).
[17] K. Hasebe, A. Nakayama, and Y. Sugiyama, Phys. Rev. E **69**, 017103 (2004).
[18] K. Hasebe, A. Nakayama, and Y. Sugiyama, Phys. Rev. E **68**, 026102 (2003).
[19] G. B. Whitman, Proc. R. Soc. London, Ser. A **428**, 49 (1990).
[20] T. Nagatani, Phys. Rev. E **61**, 3564 (2000).
[21] M. C. Cross and P. C. Hohenberg, Rev. Mod. Phys. **65**, 851 (1993).
[22] S.-Q. Dai, Adv. Mech. **12**, 2 (1982) (in Chinese).
[23] T. Nagatani, Phys. Rev. E **58**, 4271 (1998).
[24] A. H. Nayfeh, *Introduction to Perturbation Technique* (Wiley, New York, 1981).